Science with the Hubble Space Telescope – II
Space Telescope Science Institute, 1996
P. Benvenuti, F. D. Macchetto, & E. J. Schreier, eds.

Analysis of HST and IUE Spectra of β Cephei Stars

H. Cugier, M. Burghardt, D. Nowak and G. Polubek

Astronomical Institute of the Wrocław University, Kopernika 11, 51-622 Wrocław, Poland, E-mail:cugier@astro.uni.wroc.pl

Abstract. We discuss new diagnostic possibilities that follow from the identification of the driving mechanism for β Cephei stars. Two stars, δ Ceti and σ Scorpii are considered. We found that stellar models obtained from nonadiabatic observables fit other observational data very well. We also found that stellar models calculated for OPAL opacities with X = 0.70, Y = 0.28 and Z = 0.02 are in good agreement with observed properties of δ Cet and σ Sco. On the other hand, OP models which predict higher effective temperatures will result in a worse fit to the ground-based and UV spectrophotometric observations. The basic mean stellar parameters are also derived for δ Cet and σ Sco.

1 Introduction

Recent stability surveys for stellar models corresponding to β Cephei stars leave no doubt that κ–mechanism is responsible for the origin of pulsation of these stars, cf. Dziembowski (1995) and references cited therein. Cugier, Dziembowski & Pamyatnykh (1994) compared the prediction of the linear nonadiabatic theory for the amplitude ratios and the phase differences—*the nonadiabatic observables*—with multicolor photometry and radial velocity data. The agreement is satisfactory and, in most cases, the harmonic degree, l, of oscillations can be determined. Furthermore, the effect of using OP opacities (Seaton et al., 1994) instead of OPAL opacities (Rogers & Iglesias, 1992) demonstrates the usefulness of β Cephei stars to test stellar opacities. This requires accurate $T_{\rm eff}$ and metal abundance values obtained from spectroscopy.

In this paper we address these questions. Both the nonadiabatic observables and mean stellar parameters are investigated using $uvby\beta$ photometric data and UV spectrophotometric observations collected by the Goddard High-Resolution Spectrograph (GHRS) on the Hubble Space Telescope (HST) and International Ultraviolet Satellite (IUE).

2 Program stars

β Cephei stars occupy a small part of the Main Sequence band corresponding to stars with masses from 9 to 16 $M_{\odot}$. About a dozen of them (including δ Ceti and σ Scorpii) were observed by means of the IUE satellite and an extensive observational material was collected by HST/GHRS for σ Scorpii and β Canis Majoris. Here we present results for δ Cet and σ Sco, cf. Table 1. In this table we also listed mean stellar parameters derived from the Strömgren photometry and nonadiabatic observables as discussed in Sect. 3.

3 δ Ceti

IUE observational material of δ Cet consists of low and high resolution spectra obtained in modes, which do not allow us to calibrate them in the absolute units. We, therefore, constructed the mean energy flux distribution by co-adding all low resolution images for a given camera. Similarly, high

Table 1. Program stars.

Star	HD	Sp	log T_{eff} (Strömgren photometry)	log g (Strömgren photometry)	E($b-y$)	log T_{eff} (Nonadiabatic observables)	log g (Nonadiabatic observables)
δ Cet	16582	B2 IV	4.340	3.84	0.008	4.347	3.73
σ Sco	147165	B1 III	4.426	4.08	0.28	4.398	3.55

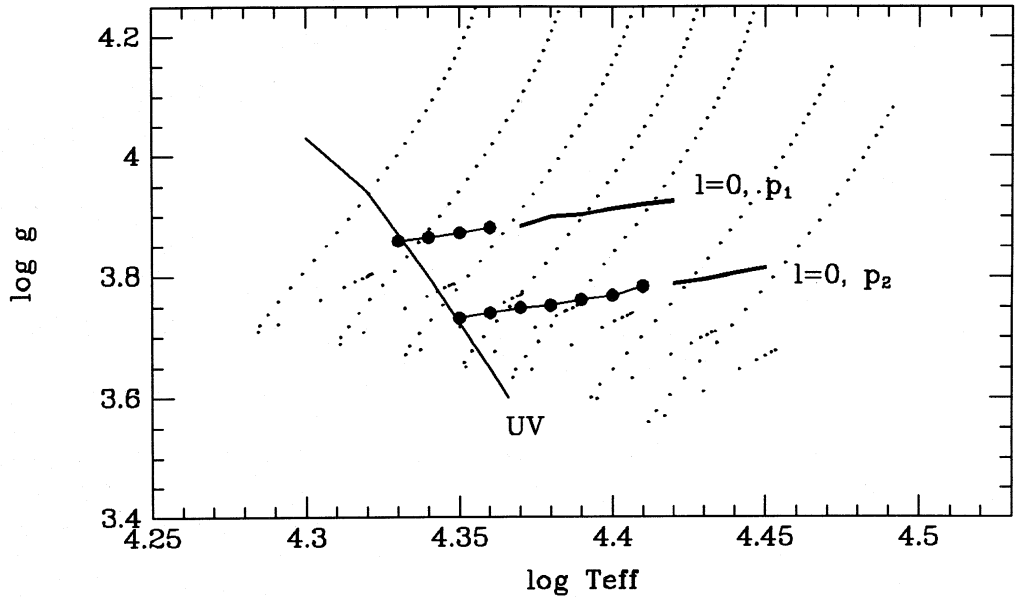

Figure 1. The diagram log g vs. log T_{eff} for stellar models of M = 8–16 $M_\odot$ during Main Sequence phase of evolution (dotted lines). Models having unstable radial modes with the period $0.^d16114$ are shown as thick lines (calculated with OP opacities) and thin lines with dots (OPAL opacities), respectively. The line marked as UV shows the best fit models to observed UV energy flux distribution.

resolution images were used to construct a mean spectrum of δ Cet because small pulsational effects for this star are not clearly seen in 0.2 Å resolution IUE data.

δ Cet is a star pulsating in the radial mode, l=0, cf. e.g., Cugier et al. (1994a). Figure 1 displays the diagram log g vs. log T_{eff} for stellar models having unstable radial modes of p_1 and p_2, with the period exactly the same as observed for δ Cet, P = $0.^d16114$. Note that models corresponding to p_1 and p_2 are shifted in log g by about 0.13 dex. Furthermore, the models calculated with OP opacities (thick lines) indicate higher effective temperature by about 0.05 dex. than OPAL (thin lines with dots) models. These model calculations are taken from Dziembowski & Pamyatnykh (1993). From the numbers given above we can conclude that knowledge of T_{eff} and log g with high precision is needed to select the correct stellar model and oscillation mode from observed period of pulsation.

An efficient method of estimating the atmospheric parameters of B-type stars is based on the Strömgren-Crawford $uvby\beta$ photometric system, cf. Nowak & Cugier (1996) for details. We found log T_{eff} = 4.340 and log g = 3.84 from data published by Lindeman & Hauck (1973), cf. Table 1. However, the observations given by Shaw (1975) lead to log T_{eff} = 4.321 and log g = 3.54. The effective temperature in the range log T_{eff} = 4.321–4.340 is in better agreement with OPAL models than OP ones.

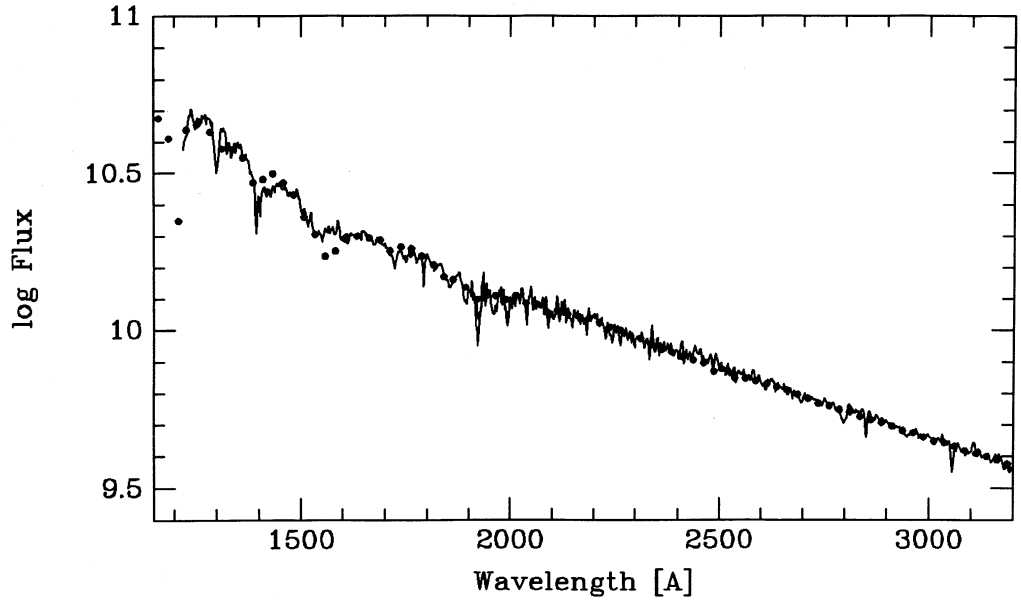

Figure 2. The best fit of the predicted flux of radiation (points) to low resolution IUE images of δ Cet (continuous line).

Next, we search for the best fit of the predicted UV radiation flux to the observed flux, by adjusting the parameters: T_{eff} and log g. The observed flux was dereddened by means of the mean extinction curve given by Savage & Mathis (1979) adopting E(B-V) = 1.26 E(b-y) + 0.007 = 0.017 mag. (cf. Nowak & Cugier 1996). Figure 2 shows the best-fit solution, but almost the same quality fits, in the sense of the χ^2–test, exist for a set of models marked as UV in Fig. 1. Again, OPAL models for stellar pulsation are in good agreement with UV flux distribution of δ Cet.

The nonadiabatic observables of δ Cet mentioned in Section 1 indicate that only p_2 mode is able to describe all observables. The best fit solution exists for OPAL stellar model with log T_{eff} = 4.347 and log g = 3.73, cf. Cugier et al. (1994a,b).

Finally, we used high resolution IUE images of δ Cet to study line profiles of selected species, namely: H I 1216, C III 1175, 1247, Si III 1206, 1300 and Si IV 1400 Å. The results plotted in Fig. 3 indicate solar abundances of Carbon and Silicon. Moreover, the calculated photospheric line profile of Ly_α is slightly weaker than the observed profile indicating interstellar absorption, cf. Fig. 3*a*. We found the Hydrogen column density towards δ Cet to be N(H I) = 1.0 10^{20} cm^{-2}.

4 σ Scorpii

The IUE observational material of σ Sco contains 62 images and a half of them were obtained in the large entrance aperture mode. Both, UV energy flux distribution and UV light curves are available for this star. Table 2 shows the observed amplitudes and moments of the maximum light at selected wavelength ranges adopting P = $0.^d246836$ for the dominant mode of pulsation according to Jerzykiewicz & Sterken (1984).

The HST/GHRS observations of σ Sco consists 31 pieces of UV spectrum taken on 9 October 1992 at wavelength region from 1127 Å to 2611 Å. A few of them are obtained in the FP-SPLIT = DSFOUR mode with 4 subexposures taken for different grating (G160M and ECH-B) positions. Both an intrinsic stellar spectrum and fixed pattern noise (FPN) are shifted relative to each other by different amounts in subexposures. We analyze these spectra using a tomographic technique already applied by Lambert et al. (1994) and Lyu et al. (1995) for HST/GHRS data. Figure 4 illustrates the raw data, FPN and reduced spectrum.

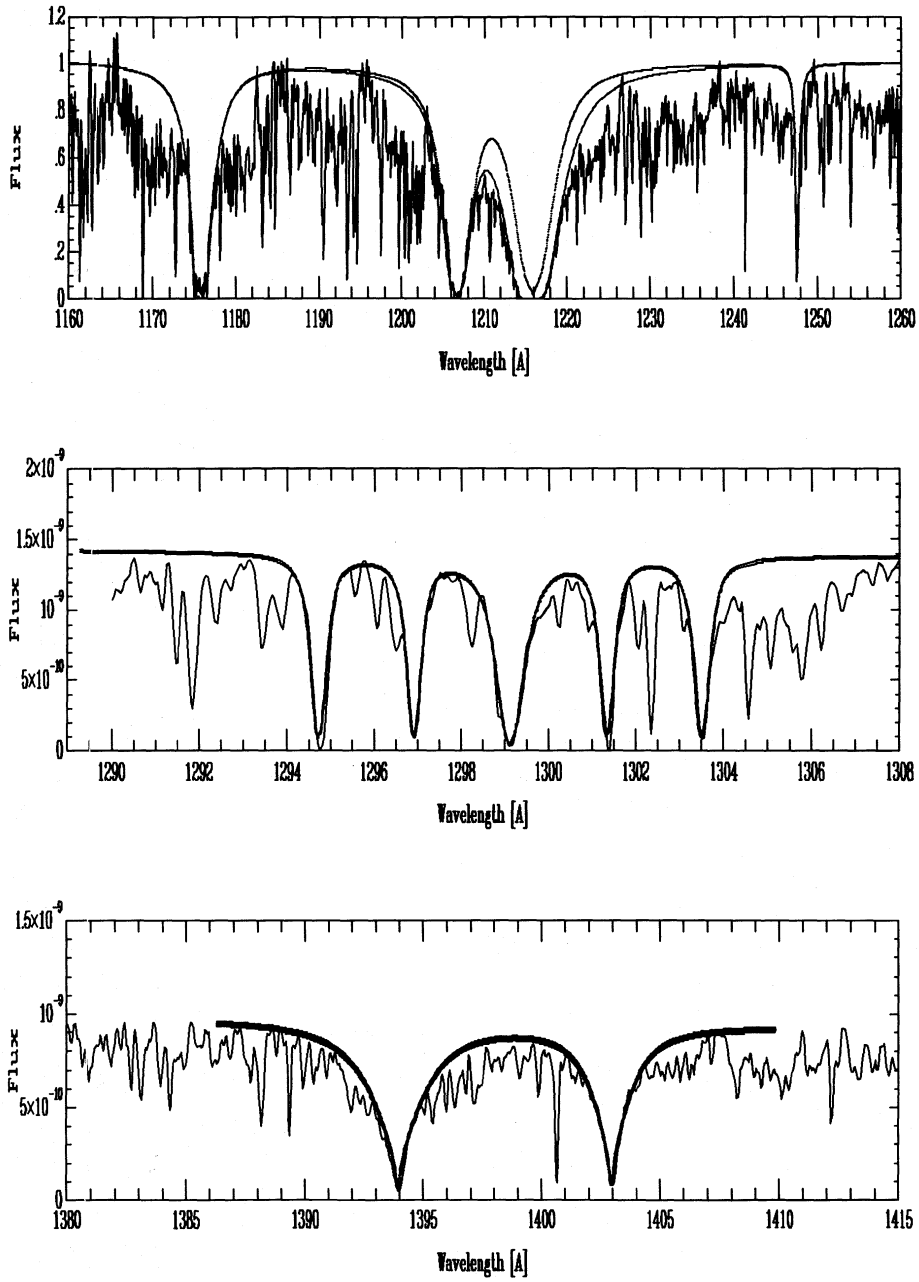

Figure 3. The high resolution IUE images of δ Cet are compared with theoretical spectra. In Panel (a) the pure photospheric spectrum is shown as dotted line, whereas the continuum line includes the effect of the interstellar absorption in Ly_{α}.

An analysis of the observed periods of oscillation and nonadiabatic observables obtained from the Strömgren photometry made by Jerzykiewicz & Sterken (1984) leads to the following stellar parameters: $M = 15.3M_{\odot}$, $\log T_{eff} = 4.3975$, $\log g = 3.55$, $R = 11.10R_{\odot}$ and $l = 0$ for the dominant mode of pulsation. These values for $\log T_{eff}$ and $\log g$ differ markedly from the results obtained from $uvby\beta$ colors shown in Table 1. We found, however, that the atmospheric model

Table 2. Amplitudes and times of maximum lights of σ Sco.

λ [Å]	Ampl. [mag]	Time JD 2444600.+
1165–1270	0.092 ± 0.009	21.1005 ± 0.0035
1270–1330	0.112 ± 0.011	21.1046 ± 0.0035
1330–1380	0.105 ± 0.008	21.1056 ± 0.0027
1420–1470	0.094 ± 0.009	21.1012 ± 0.0034
1470–1530	0.104 ± 0.008	21.1026 ± 0.0027
1570–1620	0.087 ± 0.006	21.1031 ± 0.0025
1620–1700	0.075 ± 0.007	21.1034 ± 0.0032
5500 (FES)	0.021 ± 0.004	20.9908 ± 0.0095

obtained from nonadiabatic observables fits best the HST/GHRS observations. The essentially solar abundances of Carbon and Silicon is indicated for σ Sco, cf. Fig. 5.

5 Conclusions and Discussion

Pulsation data for β Cephei stars are an important source of information about these objects. These data consist of periods of oscillations and nonadiabatic observables. The latter quantities are related to the eigenfunctions of nonadiabatic oscillations (cf. Cugier et al. 1994a).

In this paper we consider two well-known stars: δ Cet and σ Sco. We find (cf. also Cugier et al. 1994b, where BW Vul is considered) that stellar models derived from the oscillation parameters fit very well the observed UV energy flux distributions as well as line profiles taken in the high resolution mode. Figure 1 illustrates that these complementary observations are useful to distinguish between stellar opacities used in the nonadiabatic model calculations. We found that OPAL models with Z = 0.02 fit best the observed properties of δ Cet and σ Sco. On the other hand, OP models predict higher effective temperatures and will result in a worse fit to the observations.

A correctly identified nonadiabatic model means that all basic stellar (mass, age and chemical composition) parameters are known. Thus, the data on individual β Cephei stars may be used for precise determination of distances and ages of stellar systems they live in.

Having determined dominant modes of oscillation and important constraints on the mean stellar parameters, we could also derive of the chemical composition of β Cephei stars. This provides an independent test for stellar opacities. We found essentially solar abundances for Carbon and Silicon in both stars.

Finally, high signal-to-noise HST/GHRS data (cf. Figs. 4 and 5) can also be used to study dynamical effects due to stellar pulsations. Small discrepancies in the cores of the Si IV lines (cf. Fig. 5) are probably the result of such effects.

Acknowledgments. We would like to acknowledge ST-DADS and HST/ESO/CFHT Archive Services for the Space Telescope Data. STARCAT interface developed by ST-ECF, CADC and ESO has been installed on SPARCstation 2 computer at AI WrU. ESA IUE Observatory at VILSPA provided the IUE tapes. To them all we express our thanks.

This work was supported by the research grant No. 2 P03D 001 08 from the Polish Scientific Research Committee (KBN).

References

Cugier, H., Dziembowski, W. & Pamyatnykh, A. 1994a, A&A, 291, 143

Cugier, H., Pigulski, A., Polubek, G., & Monier, R. 1994b, in *Pulsation, Rotation and Mass Loss in Early-Type Stars*, IAU Symposium 162, eds. L. Balona, H. Henrichs, & J.M. LeContel (Dordrecht, Kluwer), p. 17

Dziembowski, W. 1995, in *Astrophysical Applications of Powerful New Databases*, ASP Conference Series, Vol. 78, eds. S.J. Adelman & W.L. Wiese, p. 275

Dziembowski, W. & Pamyatnykh, A.A. 1993, MNRAS, 211, 297

Jerzykiewicz, M. & Sterken, C. 1984, MNRAS, 211, 297

Lambert, D.L., Sheffer, Y., Gilliland, R.L., & Federman, S.R. 1994, ApJ, 420, 756

Lindeman, E. & Hauck, B. 1973, A&AS, 11, 119

Lyu, C.-H., Bruhweiler, F.C., & Smith, A.M. 1995, ApJ, 447, 880

Nowak, D. & Cugier, H. 1996, this issue

Rogers, F.J. & Iglesias, C.A. 1992, ApJS, 79, 507

Savage, B.D. & Mathis, J.S. 1979, ARA&A, 17, 73

Seaton, M.J., Yan Y., Mihalas, D., & Pradhan, A.K. 1994, MNRAS, 266, 805

Shaw, J. 1975, A&A 41, 367

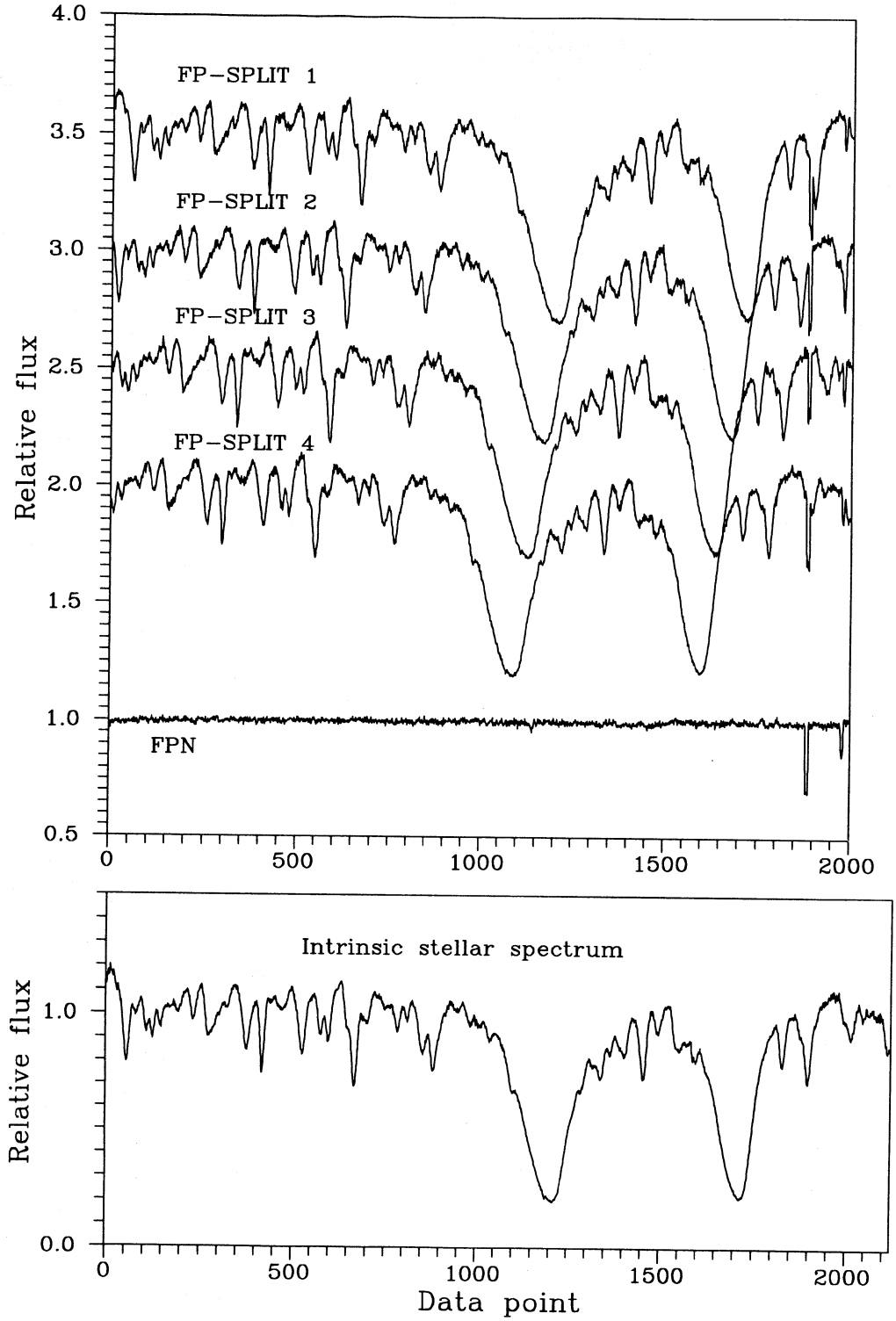

Figure 4. An example of the HST/GHRS observations of σ Sco obtained in the FP-SPLIT=DSFOUR mode. There are 4 subexposures, FPN and intrinsic stellar spectrum. FPN has an amplitude of about 0.5 percent and reveals two narrow features (blemishes) near 1900 and 2000 data point numbers.

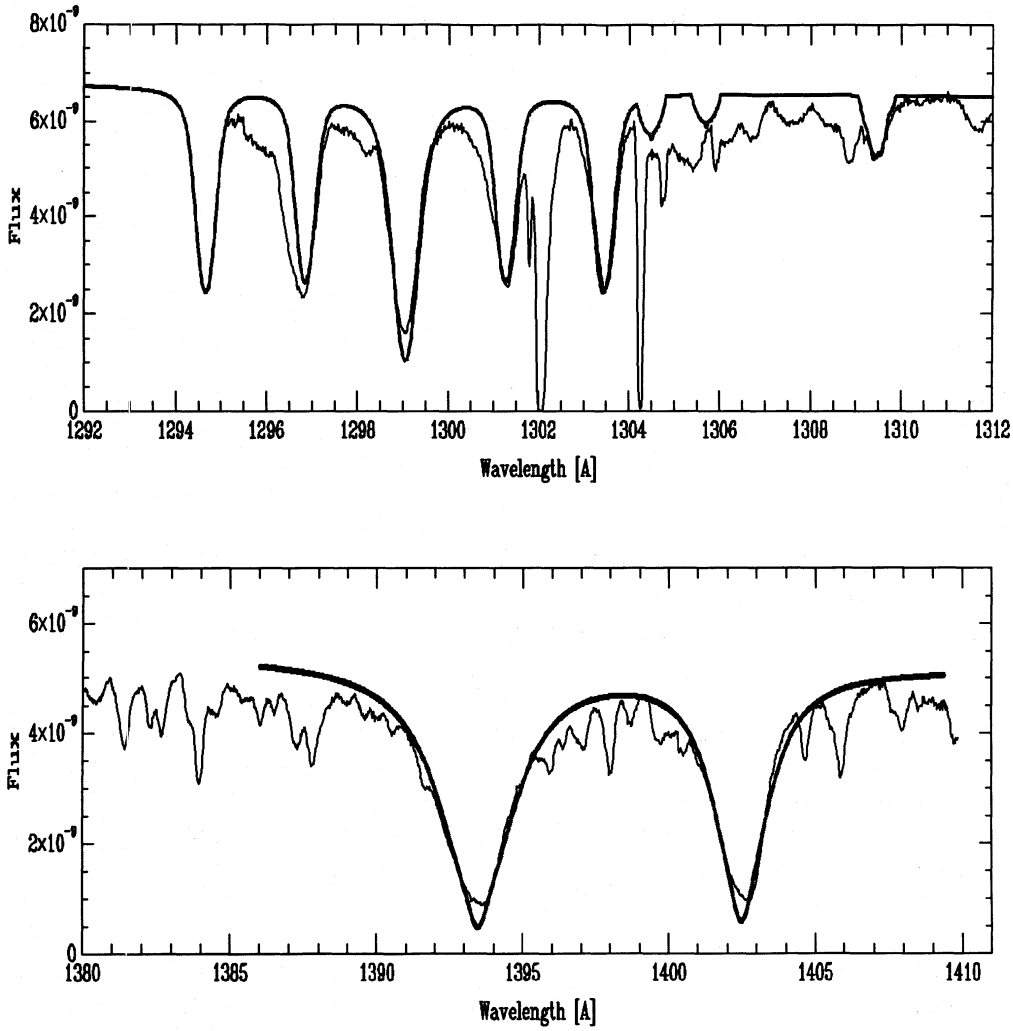

Figure 5. HST/GHRS observations of σ Sco (thin line) in comparison with spectra calculated for the photospheric model obtained from nonadiabatic observables (see text).